Korean J. Chem. Eng., 32(7), 1222-1228 (2015)
DOI: 10.1007/s11814-014-0320-z

pISSN: 0256-1115
eISSN: 1975-7220

Operation strategy of industrial crystallization for the production of 2,3,4,4′-tetrahydroxybenzophenon

Do Yeon Kim and Dae Ryook Yang†

Department of Chemical and Biological Engineering, Korea University, Seoul 136-701, Korea
(*Received 9 July 2014 • accepted 28 October 2014*)

Abstract−To improve the filterability of hydroxybenzophenone crystal, a cooling strategy for the cooling crystallization process is investigated by examining the solubility and growth kinetics of hydroxybenzophenone. The operating strategy is divided into two steps. The first step is to generate the seed by dissolving the raw material and by changing operating conditions. The second step is to grow seeds to the product with desired crystal size distribution. For each part, an operating strategy has been proposed based on the solid-liquid phase equilibrium data in a ternary system and growth kinetic experimental results. The strategy for the first step is experimentally determined under various operating conditions, and the second one is determined by theoretical modeling and model-based optimization. The average crystal size resulting from the proposed strategy has been improved and the filterability has been enhanced compared to an existing strategy used in the industry.

Keywords: Tetrahydroxybenzophenone, Crystallization, Optimization, Operation Strategy

INTRODUCTION

Tetrahydroxybenzophenone (THBP) is a light-sensitive material used in the semiconductor, cosmetic and pharmaceutical industries [8]. For the industrial applications, purified THBP is generally obtained by a batch cooling crystallization process from a mixed solvent of acetone, water and other organic solvents [2]. THBP has two types of morphology: granular- and thin needle-shaped crystals [1]. The needle-shaped crystals are preferred in the industrial production line since the granular form is an acetone solvate and, consequently, it is not suitable for purification. However, the THBP produced in the industrial processes has relatively low filterability, which leads to high cost and long operating time for downstream processes such as washing and drying because the thin needle-shaped form crystal is prone to breaking and consequently exhibits high resistance for filtering. The filterability is highly related to crystal morphology, crystal size and crystal size distribution (CSD) [7]. Thus, many researchers have investigated the crystal size, morphology and CSD to improve the filterability. However, cases of THBP purification by crystallization have not been reported to our knowledge. To obtain the improved product characteristics such as average crystal size and CSD, a cooling strategy in batch crystallization process needs to be established.

In this study, the growth kinetics and solubility of THBP dissolved in a mixed solvent of acetone and water are experimentally investigated. Based on the experimental data for the THBP-acetone-water solution, an optimized operating strategy is proposed for the batch cooling crystallization process. To verify the proposed strategy, several batch crystallization experiments were performed under different cooling strategies as well as the existing industrial strategy, and then the experimental results were compared in terms of the filterability. It is concluded that the filterability achieved by the proposed strategy is significantly improved compared to the industrial production strategy.

METHODS

1. Experimental Apparatus and Material

THBP was purified as crystals by the cooling crystallization process from a mixed solvent of water and acetone, which act as solvent and anti-solvent, respectively. The acetone (purity>99.8%) was purchased from Daejung Chemicals and Metals Co., LTD in Korea

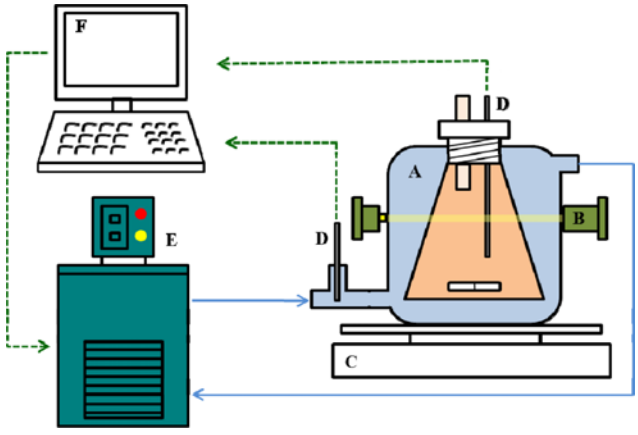

Fig. 1. Schematic diagram of the experimental apparatus.
A. Double-jacketed reactor
B. Optical sensor
C. Magnetic stirrer
D. Thermocouple
E. Bath circulator
F. Controller

†To whom correspondence should be addressed.
E-mail: dryang@korea.ac.kr
‡This paper is submitted as a contribution celebrating the honorable retirement of Prof. S.Y. Bae of Hanyang University.

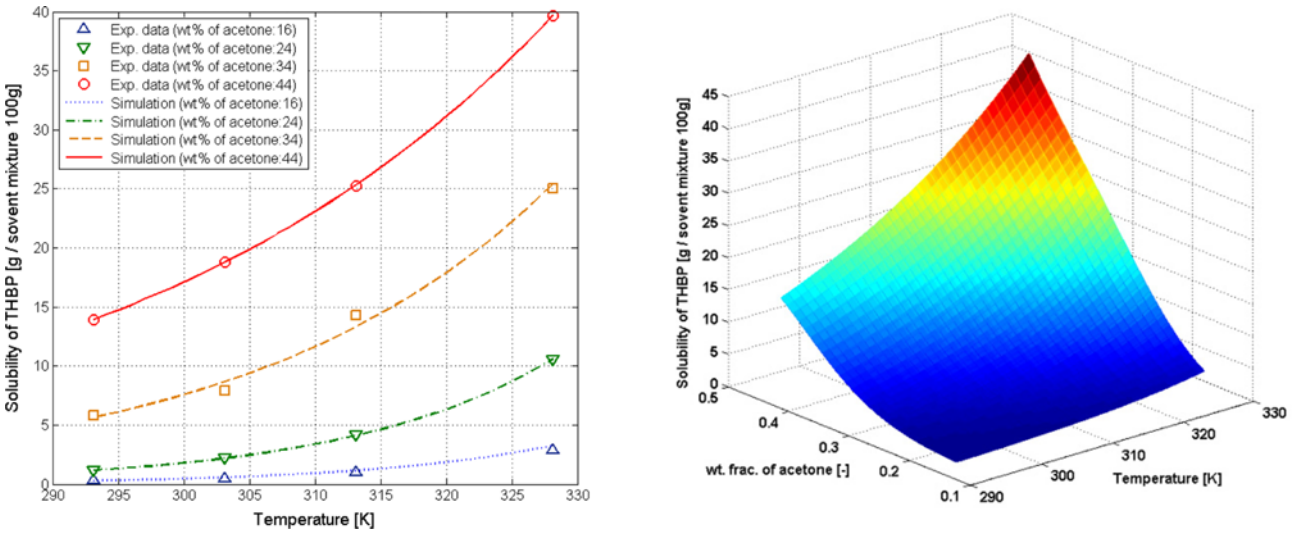

Fig. 2. Solubility of THBP.

and deionized water was used. The sample of THBP (purity>99.5%) was obtained from an actual production plant. Three types of experiments - the measurement of solubility, crystal growth rate and crystallization under each operating strategy - were conducted and an identical experimental apparatus was used for these three types of experiments, which is illustrated in Fig. 1. The reactor (A) is a 100 mL double-jacketed conical-glass flask with a Teflon screw cover with holes where a narrow glass tube and thermocouple are inserted. The glass tube was used to feed seed crystals to the reactor. Cooling water is circulated through the jacket of the reactor by the circulator (E), and two thermocouples (D), which are calibrated by the standard thermometer, measure the temperature of solution in the reactor and the cooling water in the jacket. The temperature in the reactor was controlled within the range of ±0.05 °C using a proportional-integral-derivative controller (F). The solution was agitated by the magnetic stirrer (C), and the magma density of the solution was detected by the optical sensor (B), which can indirectly measure the clouding point through the change of light intensity.

2. Solubility

The solubility of THBP in a mixed solvent of water and acetone depends on temperature and the ratio of acetone to water. Therefore, the solubility of THBP was measured from 298.15 K to 328.15 K and acetone weight fraction to solvent from 0.16 to 0.44. The gravimetrical method was used for the measurement of the THBP solubility. An excessive amount of the solute was added to the acetone and water mixture in the double-jacketed reactor whose temperature was controlled and then the suspension was agitated for 2 hours to attain equilibrium. The saturated solution was extracted by a syringe which has a filter of 0.45 μm pore size. Then, all solvent in the extracted solution was evaporated in a vacuum oven and only the remaining dried solutes were measured. The solubility can be calculated through the mass change between the extracted solution and the dried solute. The experimental solubility data are well correlated with the following expression which is a function temperature.

$$\ln(C_s)=\kappa_1 T+\kappa_2 \quad (1)$$

Table 1. Parameters for the THBP solubility correlation

Parameter	α_i	β_i	γ_i	δ_i
Value for κ_1	2.9905	−2.7805	6.5891e-1	2.3539e-2
Parameter	α_2	β_2	γ_2	δ_2
Value for κ_2	−9.0384e+2	8.1412e+2	−1.7048e+2	−1.1743e+1

where C_s is the saturated concentration of THBP and T the solution temperature. Parameters, κ_1 and κ_2, are dependent on the weight fraction of acetone to solvent and can be expressed by a polynomial form.

$$\kappa_i=\alpha_i w^3+\beta_i w^2+\gamma_i w+\delta_i \quad (2)$$

$$w=\frac{M_{acetone}}{M_{water}+M_{acetone}} \quad (3)$$

Fig. 2 shows the measured solubility and calculated results from the solubility model. The results from the solubility model have good agreement with the experimental data. The parameters used in the model are shown in Table 1.

3. Growth Kinetics

Crystal growth rate is essential for designing an operation strategy in a crystallization process. However, it is difficult to measure the crystal growth rate of THBP since the crystal shape of THBP resembles a thin needle as shown in Fig. 3. In this study, the measurement method published by Kim and Yang [3] was adopted for measuring the THBP crystal growth rate. This method is an indirect method which can obtain an averaged growth rate. Operating conditions were kept identical for each experiment except the amount of seeds, and the nucleation point was measured. Using the experimental data, parameters introduced in a growth kinetics model were estimated, which match the points of nucleation. The model for the crystal growth rate is expressed as:

$$G=\frac{dL}{dt}=k_g\Delta C^g \quad (4)$$

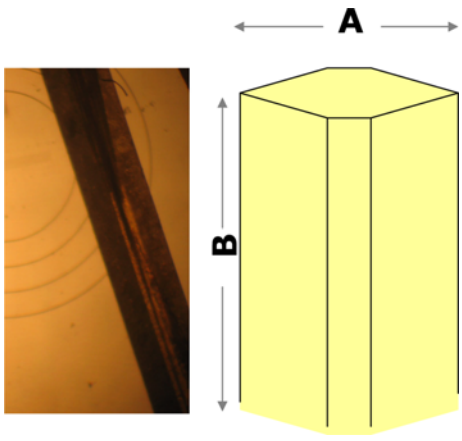

Fig. 3. Crystal shape of hydroxybenzophenone.

$$\Delta C = C - C_s \quad (5)$$

where k_g and g are growth rate constant and growth order, respectively.

Unlike an existing method which measures the growth rate of each face of crystal, this method can provide the averaged crystal growth rate by measuring the amount of solutes consumed by seeds, which is the amount of seed grown, up to the point of nucleation. This method is valid under the assumption that the nucleation occurs at the same degree of supersaturation under a constant cooling rate.

The change in the degree of supersaturation can be calculated by using the mass balance equation and the parameters for the growth kinetics can be obtained to match the measured points of nucleation as depicted in Fig. 4. The experimental data are shown in Table 2. The parameters obtained from these experimental data are k_g=0.01398 and g=1.4975.

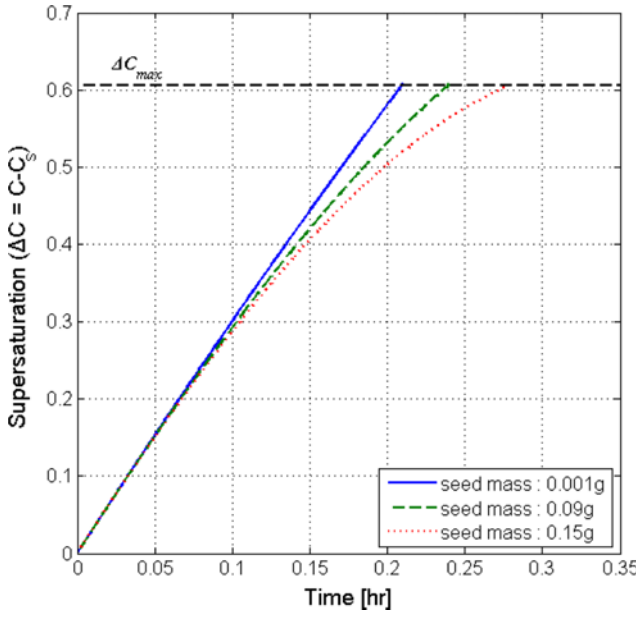

Fig. 4. The depicted nucleation points for different amount of seeds.

Table 2. Experimental data of the nucleation points for the different amount of seeds

No.	Cooling rate [K/hr]	Seed mass [g]	Nucleation point	
			[K]	[sec]
1	10	0.001	325.85	756
2	10	0.09	325.55	864
3	10	0.15	325.15	1008

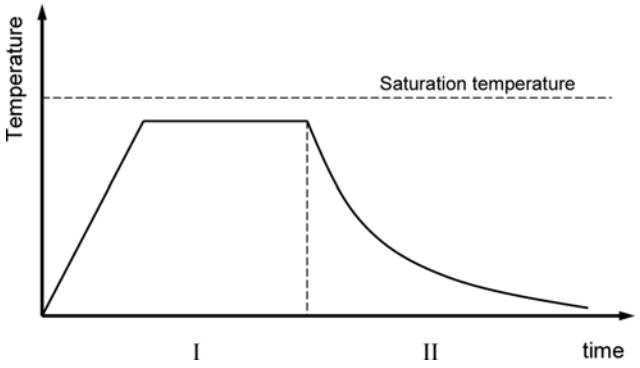

Fig. 5. Crystallization strategy in industrial process.

4. Development of Operation Strategy

THBP is purified by the batch cooling crystallization process for the industrial uses. After the synthesis process of the THBP, water, acetone and the synthesized THBP are put together and mixed in a crystallizer. Then, the mixture is heated to a specific temperature which lies below its saturation temperature in order to leave some THBP crystals un-dissolved, which play a role as seeds in the next cooling step. Fig. 5 shows the cooling crystallization strategy used in an industrial process for the production of the THBP. The crystal size distribution (CSD) and mean size are the most crucial factors among other qualitative characteristics of the crystallized product due to their influences on the performance of downstream processes such as centrifuging, washing and drying. To improve the product quality, a two-step method is proposed in this study, for which the operating conditions need to be optimized. The first step is to generate the seeds by dissolving a raw material in an optimized operating condition, the seed preparation step. The objective of this step is to obtain well-shaped seeds with a narrow CSD. In the second step, the seeds generated in the first step will grow and the operating conditions are controlled for the crystals to grow to the desired crystal size distribution. The second step is the crystal growth step, which aims to grow the seeds with a large mean size and narrow CSD through suppressing the nucleation. For each step, an optimal operation strategy needs to be found by using the solid-liquid phase equilibrium data in a ternary system and growth kinetic experiments. The operating strategy for the first step is experimentally determined by carrying out a number of operating scenarios, and the second one is determined by the theoretical modeling and model-based optimization.

An experimental procedure which was used to find an optimal strategy for the seed preparation step is presented in Fig. 6. Initially, the synthesized THBP solutes are mixed with only acetone in the

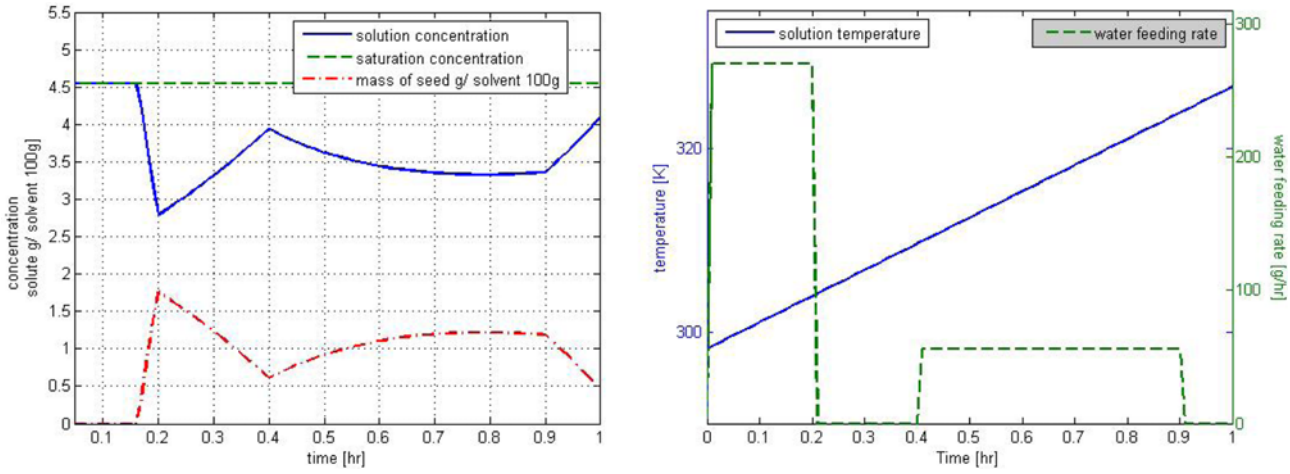

Fig. 6. Seed preparation step (Left: the solubility profile; Right: temperature profile and anti-solvent feeding rate).

crystallizer and, therefore, all the THBP solutes in crystallizer are dissolved due to the absence of anti-solvent, water. Then, water is injected periodically as the temperature increases. As shown in Fig. 6, the higher temperature rises, the higher solubility becomes. On the contrary, the solubility decreases as adding water. Therefore, the solution becomes super-saturated while water is injected and, consequently, the nucleation and crystal growth can occur. When the water injection is stopped, the solubility increases again due to the increasing temperature and the solution becomes un-saturated, which induces the dissolution of the crystals. This method is similar to 'temperature swing' and can provide well-shaped and uniform seeds.

In the crystal growth step, it is important to induce only the crystal growth without nucleation. Therefore, an optimal temperature profile which can achieve the desired condition needs to be found through model-based optimization. An objective function for the optimization is established as shown in Eq. (6), which represents the maximization of the average crystal size. The cooling rate is constrained not to exceed a fixed maximum cooling rate, which is chosen to be 50 K/hr in this study, and the degree of the supersaturation should always lie within the metastable region so as to minimize the nucleation.

$$\begin{aligned} &\underset{u(t)}{\text{Maximize}}\ J=\bar{L}(t) \\ &\text{Subject to: } 0\le u(t)\le 50 \\ &\qquad C(t)-C_s(t)\le \Delta C_{max} \end{aligned} \tag{6}$$

The temperature profile is optimized by using a population balance equation along with the phase equilibrium and growth rate kinetics. The model and optimization algorithm used is adopted from the previous study [4]. Assuming that crystal agglomeration and breakage are not present and crystal growth is not dependent on crystal size, the population balance equation (PBE) for batch crystallization is obtained as in the following form.

$$\frac{\partial f(L,t)}{\partial t}=G(t)\frac{\partial f(L,t)}{\partial L} \tag{7}$$

where f denotes the population density of crystals, t the time, L the size of the crystals, and G the crystal growth rate as shown in Eq. (4). To solve the population balance, initial and spatial boundary conditions are required as follows:

$$\begin{aligned} &f(0,t)=\frac{B}{G|_{L=0}} \quad (\text{at } \Delta C>\Delta C_{max}) \\ &f(0,t)=0 \quad (\text{at } \Delta C\le\Delta C_{max}) \\ &f(L,0)=f_0 \end{aligned} \tag{8}$$

In this study, the spatial boundary condition at L=0 for the population density of crystals can be set as shown in Eq. (8); f (0, t)=0, since it is assumed that the nucleation does not occur if the process is operated within the metastable zone. The experimental result from the seed preparation step is used as an initial boundary condition.

The population balance needs to be coupled with the mass balance. The mass balance for a batch cooling crystallizer is

$$\frac{dC}{dt}=-\rho_c k_v\frac{d\mu_3}{dt} \tag{9}$$

where ρ_c is crystal density, k_v the volume shape factor and μ_3 the

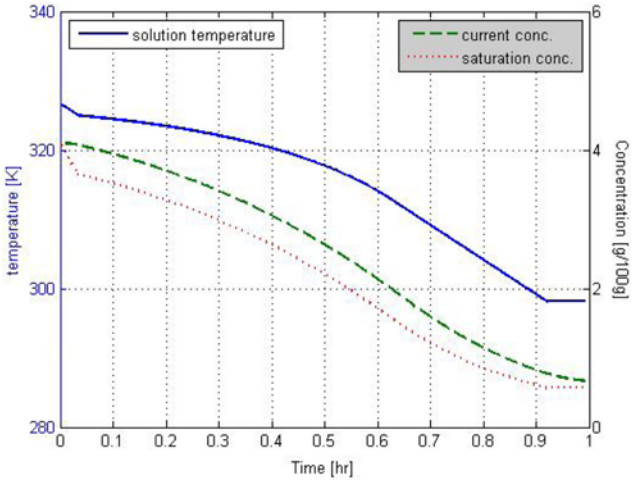

Fig. 7. The optimal temperature profile of crystal growth step.

third moment of the population density. The definition of the third moment is

$$\mu_3 = \int_0^\infty fL^3 dL \quad (10)$$

The optimal temperature profile for the crystal growth step is obtained from the above set of equations and the result is shown in Fig. 7.

RESULTS AND DISCUSSION

To evaluate the performance of the proposed strategy, six operating strategies (two strategies for the seed preparation step multiplied by three cooling strategies for the crystal growth step) were conducted and experimental results were compared. For the seed preparation step, the existing industrial strategy and proposed strategy in this study were compared. For the crystal growth step, three temperature profiles (industrial, linear and optimal) were used, as shown in Fig. 9.

The generated seed crystals through the optimal strategy in the seed preparation step are shown larger and more well-shaped than those from the industrial strategy. Fig. 8 shows the images of the seed crystals taken at the end of the seed preparation step with the two different strategies. The final CSD resulting from the industrial strategy is affected by the intermediate CSD after the THBP synthesis process because the crystals from the synthesis process are incompletely dissolved and the remaining crystals are used in the next crystal growth step. However, using the proposed strategy, all crystals from the synthesis process can be dissolved, and seed crystals are prepared only by the concentration swing as described earlier. As a result, there are hardly any effects of the previous synthesis process on the seed preparation step.

The two different seed crystals produced in the first step are used for three different types of cooling strategies for the second step, which follows the industrial, linear and optimal temperature profile. All strategies have same final temperature. In the linear cooling strategy, the cooling rate is optimized while the final temperature is maintained the same as other strategies for the same productivity of crystal production.

Figs. 10-12 show the crystal products obtained by the six operation strategies. In Fig. 10, the industrial cooling strategy which has large temperature drop initially results in a large amount of fine particles regardless of seed preparation step. In Fig. 11, the linear cooling strategy with optimal seed preparation results in better product quality than the industrial cooling strategy. In Fig. 12, the optimal cooling strategy with optimal see preparation results in the best product quality. From these results, the cooling strategy seems to be more important than the seed preparation strategy.

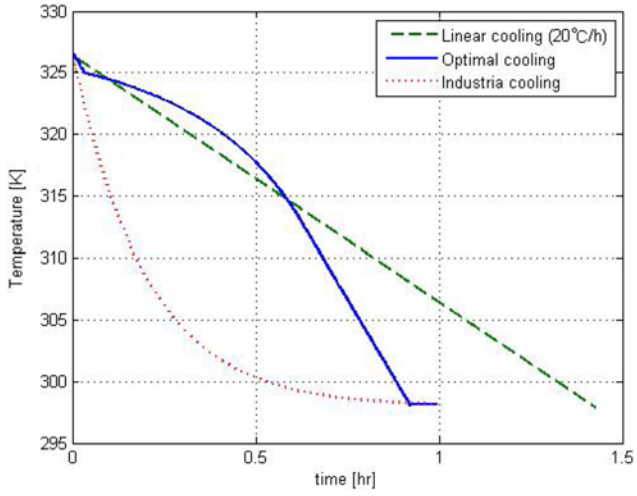

Fig. 9. Three types of temperature profile.

To compare the performance of the six strategies quantitatively, the filterability of the final products produced has been measured experimentally. The filterability can represent the performance of the crystallization process in this study because it is highly related to the performance of downstream processes such as centrifuging, washing and drying [6]. If the product crystals have good filterability, that means less amount of purified water and energy is consumed for washing and drying, respectively. At a constant filtration pressure, the following equations can be applied for the filterability, which can be represented by cake resistance, α [5].

$$t = \frac{\mu}{g_c(-\Delta P)}\left[\frac{c\alpha}{A}\left(\frac{V}{A}\right)^2 + R_m\frac{V}{A}\right] \quad (11)$$

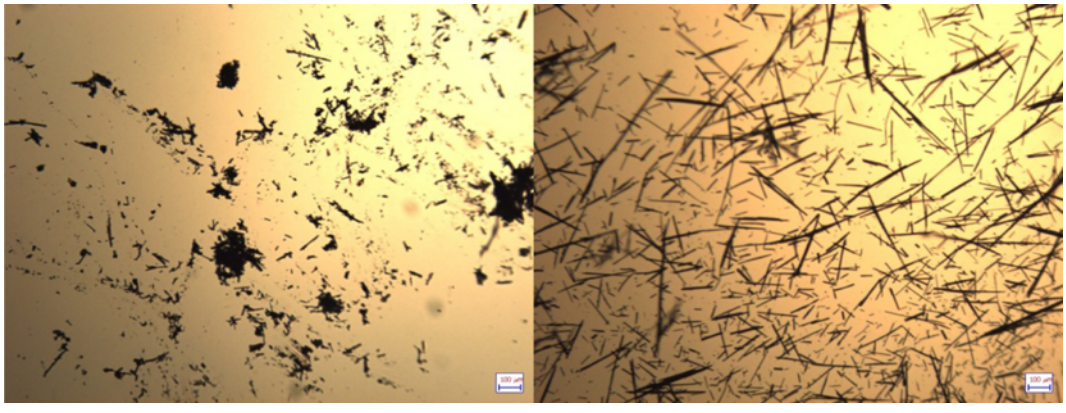

Fig. 8. Crystals from industrial (left) and optimal (right) strategy for seed preparation.

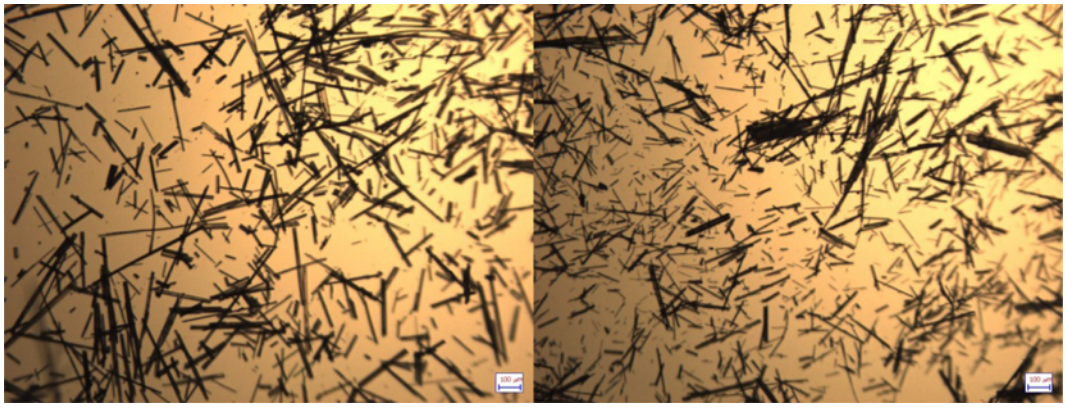

Fig. 10. Results of industrial cooling strategy (Left: with industrial seed preparation, right: with optimal seed preparation).

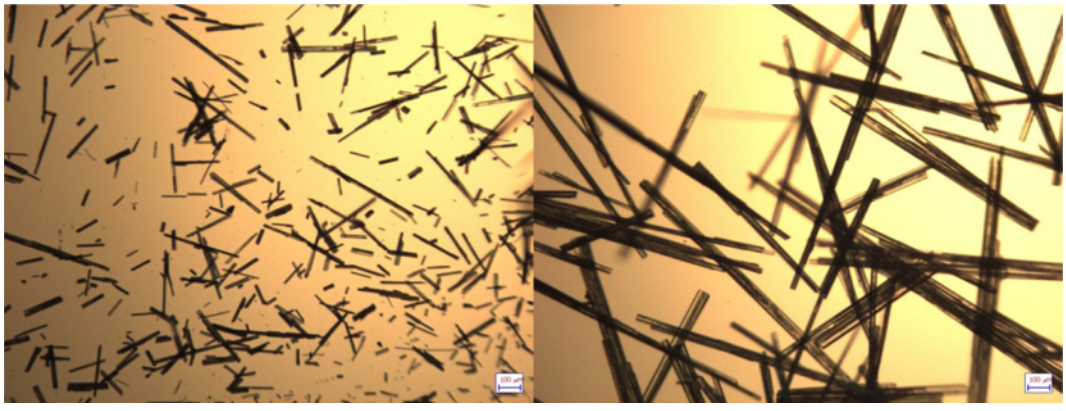

Fig. 11. Results of linear cooling strategy (20 °C/hr) (Left: with industrial seed preparation, right: with optimal seed preparation).

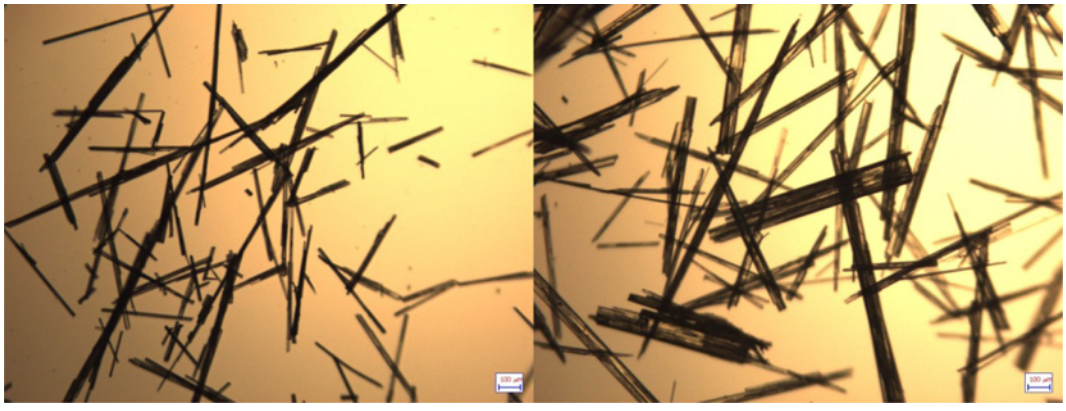

Fig. 12. Results of optimal cooling strategy (Left: with industrial seed preparation, right: with optimal seed preparation).

$$\alpha = \frac{k(1-\varepsilon)}{\varepsilon^3 \rho_p \phi^2} \tag{12}$$

where t is the total filtration time, μ the filtrate viscosity, ΔP the overall pressure difference across the filter, α the specific cake resistance, A the cake area, V the total volume of filtrate collected during the total filtration time t, R_m the filter-paper resistance, ε the cake porosity, ρ_p the particle density and ϕ the particle sphericity. In this study, the total filtration time is measured while the constant pressure difference and filtrated volume are maintained with the same type of filter paper, which gives the same filter-paper resistance R_m. For comparison, a relative cake resistance normalized by the cake resistance of the products from the industrial seed preparation and industrial cooling strategy is used. Table 3 presents the experimental results of the relative cake resistance. The lower value of relative cake resistance indicates better filterability as shown in Eq. (11). From the experimental results, the proposed optimal strategy (the combination of the optimal seed preparation and optimal cooling) shows the best performance for the filterability. The optimal cooling strategy in the second step shows improved performance regard-

Table 3. Experiment results of the relative cake resistance

Step		Experimental filtration time [sec]				Relative cake resistance [-]
Seed preparation	Crystal growth	Exp. #1	Exp. #2	Exp. #3	Avg.	
Industrial	Industrial	26.94	28.22	28.39	27.85	1.0000
Industrial	Linear	18.29	18.88	18.84	18.67	0.4700
Industrial	Optimal	16.43	15.83	16.17	16.14	0.3241
Optimal	Industrial	36.77	38.12	37.05	37.31	1.5464
Optimal	Linear	12.86	13.55	13.36	13.26	0.1574
Optimal	Optimal	11.21	11.35	11.82	11.46	0.0537

less of seed preparation step. Also, the optimal seed preparation strategy enhances the filterability except for the case of industrial cooling strategy, as similarly illustrated in the pictures above. This result confirms the observation in Figs. 10-12, which show that the cooling strategy is more important than the seed preparation step.

CONCLUSIONS

An optimal cooling strategy of the THBP production has been developed. For the seed preparation step, an empirical method is devised to exploit the solubility swing effect by adding an anti-solvent. For the crystal growth step, an optimal cooling strategy has been obtained by solving a model-based optimization problem using the population balance model while imposing the constraints of maximum cooling rate and degree of super-saturation. From the images of the final products obtained from a microscopic analysis, it can be concluded that the combination of the optimal seed preparation and optimal cooling method provides large and well-shaped crystal products compared to the existing methods. For quantitative comparisons, the relative filterability is measured and the proposed method achieves highly enhanced filterability than does the industrial method.

ACKNOWLEDGEMENTS

This work was supported by the Human Resources Development program (No. 20134010200600) of the Korea Institute of Energy Technology Evaluation and Planning (KETEP) grant funded by the Korea government Ministry of Trade, Industry and Energy, and also by Korea University.

REFERENCES

1. M. Itoh, Y. Kuniyoshi, M. Yokota, N. Doki and K. Shimizu, *J. Chem. Eng. Data*, **52**, 2484 (2007).
2. M. Itoh, Y. Kuniyoshi, M. Yokota, N. Doki and K. Shimizu, *Organic Process Research Development*, **12**, 655 (2008).
3. D. Y. Kim and D. R. Yang, *J. Cryst. Growth*, **373**, 54 (2013).
4. D. Y. Kim, M. Paul, J. Repke, G. Wozny and D. R. Yang, *Korean J. Chem. Eng.*, **26**, 1220 (2009).
5. W. L. McCabe, J. C. Smith and P. Harriott, *Unit Operations of Chemical Engineering*, 5th Ed. McGraw-Hill (1993).
6. M. Mirmehrabi, S. Rohani, K. S. K. Murthy and B. Radatus, *J. Pharm. Sci.*, **93**, 1692 (2004).
7. P. J. Jansens, Y. H. M. Langen, E. P. G. van den Berg and R. M. Geertman, *J. Cryst. Growth*, **155**, 126 (1995).
8. K. Yamasaki1, H. Okuda and H. Kikkawa, *J. Clinical Toxicology*, **2** (2012).